AJNR

Dynamic CTA-Derived Perfusion Maps Predict Final Infarct Volume: The Simple Perfusion Reconstruction Algorithm

C.C. McDougall, L. Chan, S. Sachan, J. Guo, R.G. Sah, B.K. Menon, A.M. Demchuk, M.D. Hill, N.D. Forkert, C.D. d'Esterre and P.A. Barber

AJNR Am J Neuroradiol 2020, 41 (11) 2034-2040
doi: https://doi.org/10.3174/ajnr.A6783
http://www.ajnr.org/content/41/11/2034

Dynamic CTA-Derived Perfusion Maps Predict Final Infarct Volume: The Simple Perfusion Reconstruction Algorithm

C.C. McDougall, L. Chan, S. Sachan, J. Guo, R.G. Sah, B.K. Menon, A.M. Demchuk, M.D. Hill, N.D. Forkert, C.D. d'Esterre, and P.A. Barber

ABSTRACT

BACKGROUND AND PURPOSE: Infarct core volume measurement using CTP (CT perfusion) is a mainstay paradigm for stroke treatment decision-making. Yet, there are several downfalls with cine CTP technology that can be overcome by adopting the simple perfusion reconstruction algorithm (SPIRAL) derived from multiphase CTA. We compare SPIRAL with CTP parameters for the prediction of 24-hour infarction.

MATERIALS AND METHODS: Seventy-two patients had admission NCCT, multiphase CTA, CTP, and 24-hour DWI. All patients had successful/quality reperfusion. Patient-level and cohort-level receiver operator characteristic curves were generated to determine accuracy. A 10-fold cross-validation was performed on the cohort-level data. Infarct core volume was compared for SPIRAL, CTP–time-to-maximum, and final DWI by Bland-Altman analysis.

RESULTS: When we compared the accuracy in patients with early and late reperfusion for cortical GM and WM, there was no significant difference at the patient level (0.83 versus 0.84, respectively), cohort level (0.82 versus 0.81, respectively), or the cross-validation (0.77 versus 0.74, respectively). In the patient-level receiver operating characteristic analysis, the SPIRAL map had a slightly higher, though nonsignificant ($P < .05$), average receiver operating characteristic area under the curve (cortical GM/WM, $r = 0.82$; basal ganglia = 0.79, respectively) than both the CTP–time-to-maximum (cortical GM/WM = 0.82; basal ganglia = 0.78, respectively) and CTP-CBF (cortical GM/WM = 0.74; basal ganglia = 0.78, respectively) parameter maps. The same relationship was observed at the cohort level. The Bland-Altman plot limits of agreement for SPIRAL and time-to-maximum infarct volume were similar compared with 24-hour DWI.

CONCLUSIONS: We have shown that perfusion maps generated from a temporally sampled helical CTA are an accurate surrogate for infarct core.

ABBREVIATIONS: AUC = area under the curve; EVT = endovascular therapy; mCTA = multiphase CTA; ROC = receiver operating characteristic; SPIRAL = simple perfusion reconstruction algorithm; Tmax = time-to-maximum

Endovascular therapy (EVT) for acute ischemic stroke can lead to remarkable results for improving stroke outcome.[1-3] The emphasis on fast treatment decisions for patients with acute ischemic stroke requires simple, quick, and accurate neuroimaging of patients for detection of early ischemic changes. Additionally, image-processing software that can provide this information should be preferably inexpensive and easily accessible to all stroke centers, both primary and comprehensive, around the world. CT is the most commonly used and practical imaging technique for assessing patients with acute stroke, but sensitivity and reliability are only modest, even in the hands of stroke specialists. Software systems, including perfusion analysis, to identify ischemic tissue using advanced imaging paradigms are now recommended by the American Stroke Association and have been used successfully in several clinical trials, including selection of patients for EVT up to 24 hours after stroke.[4-6]

Received April 21, 2020; accepted after revision July 7.

From the Department of Clinical Neurosciences (C.C.M., R.G.S., B.K.M., A.M.D., M.D.H., C.D.d., P.A.B.), Calgary Stroke Program; Department of Radiology (C.C.M., B.K.M., N.D.F., C.D.d.E., P.A.B.); Hotchkiss Brain Institute (C.C.M., B.K.M., A.M.D., M.D.H., N.D.F., C.C.d.E., P.A.B.); and Department of Clinical Neurosciences (C.C.M., L.C., S.S., J.G., R.G.S., B.K.M., A.M.D., M.D.H., N.D.F., C.C.d.E.); Alberta Children's Hospital Research Institute (N.D.F.), University of Calgary, Calgary, Alberta, Canada; and Seaman Family Centre (C.C.M., R.G.S., B.K.M., A.M.D., M.D.H., C.D.d.E., P.A.B.), Foothills Medical Centre, Calgary, Alberta, Canada.

This work was supported by the Heart and Stroke Foundation of Canada by a grant-in-aid for the REPERFUSE study.

Please address correspondence to Philip A. Barber, MB, ChB, MD, FRCP (Edinburgh), FRCPC, Calgary Stroke Program, Department of Clinical Neurosciences, University of Calgary, 3330 Hospital Dr NW, Calgary, AB T2N 4N1, Canada; e-mail: pabarber@ucalgary.ca

http://dx.doi.org/10.3174/ajnr.A6783

Infarct core volume measurement using CTP at patient admission is the mainstay for stroke-treatment decision-making.[4,6,7] CTP improves the detection of ischemia, contributing to the improved accuracy for stroke diagnosis.[8] Also, there are several potential downfalls with cine CTP technology, which include increased radiation dose to the patient; an extra bolus of CT contrast agent, which could cause renal complications; the additional time to acquire and process the perfusion data; the requirement of expensive software and licenses; the lack of standardization across vendor platforms; and limited craniocaudal coverage, to name a few. Therefore, there is a pressing need to improve the accessibility and practicality of brain perfusion imaging while maintaining the diagnostic and prognostic accuracy for radiologic outcome (final infarct volume).

The simple perfusion reconstruction algorithm (SPIRAL) described in this article is a method for analyzing low-temporal-resolution, contrast-enhanced, spiral/helical CT brain scans to obtain perfusion parameter maps of the brain, providing perfusion maps comparable with a cine CTP acquisition for predicting infarct core. Using a group of patients undergoing endovascular treatment with successful reperfusion, we sought to determine the accuracy of SPIRAL perfusion and CT perfusion images for follow-up of infarction confirmed on 24- to 48-hour diffusion-weighted MR imaging.

MATERIALS AND METHODS

Patients

A post hoc analysis was performed using data from the Measuring Collaterals With Multi-phase CT Angiography in Patients With Ischemic Stroke (PRove-IT) and Endovascular Treatment for Small Core and Proximal Occlusion Ischemic Stroke (ESCAPE) studies from the Calgary Stroke Program.[1,9] Patients with acute ischemic stroke were included in the study if they presented within 12 hours from last seen healthy. Inclusion criteria for the present study were as follows: 1) older than 18 years of age; 2) known symptom-onset time; 3) any occlusion of the anterior circulation, which could be targeted for EVT; 4) successful reperfusion assessed by digital subtraction angiography at end of the EVT; and 5) next-day follow-up DWI between 2 and 48 hours of admission. A modified TICI score of 2b or 3 was considered successful reperfusion.[1,2] Demographic and clinical characteristics, medical history, and any relevant workflow time intervals were collected prospectively. The study was approved by the local ethics board of The University of Calgary.

Image Acquisition

At admission, all patients had a standard NCCT scan (5-mm section thickness), a head/neck multiphase CTA (mCTA), and cine CTP with a craniocaudal coverage of 8 cm. The mCTA acquisition has been described previously.[9] Briefly, 80 mL of an iodinated contrast agent was injected at a rate of 5 mL/s followed by a saline flush of 50 mL at 6 mL/s. For the first phase (7 seconds), the aortic arch-to-vertex helical scan was timed to be in the peak arterial phase by triggering the scan with contrast bolus tracking. The second phase was acquired after a delay of 4 seconds, allowing the table to reposition to the skull base. Scan duration for the next 2 additional phases was 3.4 seconds. Images were reconstructed into 0.625-mm section thickness. For the cine CTP protocol, 45 mL of CT contrast agent (ioversol, Optiray 320; Mallinckrodt) was power-injected at 4.5 mL/s followed by a saline chase of 40 mL at 6 mL/s. Sections of 8-cm thickness were acquired at 5-mm section thickness. Scanning began after a delay of 5 seconds from contrast injection in up to 2 phases (scanning intervals): the first phase every 2.8 seconds for 60 seconds and an additional second phase every 15 seconds for 90 seconds (total scan time = 150 seconds).

Between 24 and 48 hours of treatment, a clinical DWI scan was acquired using 3T MR imaging (Signa VH/i; GE Healthcare) (flip angle = 90°, single-shot echo-planar sequence, $b = 0$ s/mm^{-2} and isotropic $b = 1000$ s/mm^{-2}, TR = 9000 ms, TE = minimum [80–90 ms], FOV = 240 mm, section thickness = 5.0 mm with a 0- or 2-mm gap).

Image Processing

SPIRAL Perfusion Functional Map Processing. To generate SPIRAL functional images, we registered each phase of the mCTA to the NCCT using a rigid registration. The NCCT was used to determine the baseline Hounsfield unit for each region of the brain in a respective patient. The dynamic series generated from the NCCT and mCTA was postprocessed with the following steps: 1) The skull and ventricles were removed using per-patient Hounsfield unit thresholds on the NCCT (ventricles = 0–12 HU, skull > 60 HU). Time-attenuation curves were created for each voxel after subtraction of the baseline NCCT Hounsfield unit values, a normalization technique common in perfusion processing.[7] Deconvolution and nondeconvolution approaches were used to generate functional maps of TTP or T0 (time to peak of impulse residue function), CBF, MTT, and CBV.[7,10] Singular-value decomposition deconvolution was performed for each tissue voxel after selection of an arterial input function from the internal carotid artery.[7] For the nondeconvolution approach, we created 5 hemodynamic functional maps: 1) TTP = the mCTA phase with the highest magnitude Hounsfield unit; 2) phase 1 blood flow = the slope of the first and second Hounsfield unit magnitudes from the mCTA; 3) phase 2 blood flow = the slope of the second and third Hounsfield unit magnitudes from the mCTA; 4) flow average = the average of 2 and 3; 5) blood volume = integral of the of time-attenuation curves. For all deconvolution and nondeconvolution functional maps, collinearity was determined with a variance inflation factor; any metric with a variance inflation factor of >4 was removed from the analysis. A backward stepwise logistic regression model was trained using the remaining functional maps to create the SPIRAL functional map. The logistic regression coefficients were varied inside an exponential function to iteratively evaluate the discriminatory ability of the model to distinguish infarction and noninfarction at a voxel-level. The equation that is fit to the data is shown below:

$$P = \frac{1}{1 + e^{-(A + BX + CY + DZ + EW)}},$$

where P is the probability of a binomial outcome (between 0 and 1), A is a scaling constant, X and B are the TTP map and the corresponding coefficient, Y and C are the CBF map and the corresponding coefficient, Z and D are the MTT map and the corresponding coefficient, and E and W are the deconvoluted T0 map and associated coefficient.

Perfusion Functional Map Processing. In a subset of 40 patients, CTP functional maps were processed by an expert (C.D.d.E.)

using commercially available deconvolution software (CT Perfusion 4D; GE Healthcare). For each study, the arterial input function was manually selected from the basilar artery or contralateral ICA using a 2 voxel × 2 voxel (in-section) ROI. For all arterial input functions, baseline-to-peak height Hounsfield unit differences matched those from the respective sagittal sinus. Absolute maps of cerebral blood flow [mL × min^{-1} · $(100\ g)^{-1}$] × MTT (seconds) start time of the impulse residue function (ie, delay of the tissue time-density curve with respect to the arterial input function) (T0; second) and time-to-maximum (Tmax) = T_o + 0.5 × MTT (seconds) were calculated by deconvolution of tissue time-density curves and the arterial input function using a delay-insensitive algorithm (CT Perfusion 4D). Average maps were created by averaging the serial (dynamic) CTP images over the duration of the first pass of contrast; these average maps have suitable anatomic detail for gray/white matter segmentation and as the source image for registration with follow-up imaging. In-plane patient motion was corrected in the x-/y-axis using automated software (CT Perfusion 4D), and in cases with extreme motion, time points were manually removed as needed.[9]

Perfusion Parameter Map Registration. All perfusion parameter maps generated from the mCTA and CT perfusion studies, respectively, were registered to the follow-up DWI dataset. Therefore, the optimal rigid transformation was computed between the follow-up DWI and average CTP or NCCT dataset, respectively, using the mutual-information image-similarity metric within a multiresolution approach.[11,12] The resulting transformations were then used to transform the perfusion parameter maps to the follow-up DWI dataset using linear interpolation.

Infarct Segmentation and Perfusion Data Extraction. Delineation of the follow-up infarct volume (ROI-1) was performed on the follow-up DWI by applying a single standardized intensity.[13] A noninfarct ROI (ROI-2) encompassed any brain tissue outside ROI-1, including voxels from the contralateral hemisphere. Subcortical structures (ie, basal ganglia, including the caudate, lentiform, and internal capsule) were manually segmented and analyzed separately from cortical gray/white matter.

Histograms were generated for all ROI-1 and ROI-2 segmentations, respectively, from the SPIRAL perfusion image and CTP Tmax and CBF maps because these maps have been previously shown by the authors to have the highest accuracy for final infarction.[7] Patient-level histograms from ROI-1 and -2 were amalgamated to create a single "all patient" ROI-1 and ROI-2 to perform a cohort-level analysis.

An additional analysis was undertaken to evaluate the effect of lesion size on the SPIRAL lesion-detection method described. Lesions at different size intervals were chosen, while larger or smaller lesions were eliminated from the analysis. This interval mean was shifted from 0.015 to 1000 mL, with the upper and lower bounds on the interval being 10% of the mean (ie, 100 -mL mean, 90- to 110-mL interval). This analysis was completed to determine whether smaller petechial lesions were not identified by the SPIRAL algorithm.

Statistical Analysis

Clinical data were summarized using standard descriptive statistics. We performed a patient-level analysis and cohort-level analysis using receiver operating characteristic (ROC) curve analysis. At the patient level, the area under the ROC curve was determined (area under the curve [AUC]) for each patient. At the cohort level, an AUC-ROC was determined for all infarct voxels and noninfarct voxels from all patients in an amalgamated histogram. The Youden method was used to determine these optimal thresholds most associated with follow-up MR imaging infarct volume along with respective sensitivities and specificities for each threshold.[14] AUC values were compared between SPIRAL and CTP-CBF and Tmax maps. Bland-Altman plots were created to compare SPIRAL, CTP Tmax, and follow-up DWI lesion volumes using the model/thresholds derived in the cohort-level analysis of 40 patients with both mCTA and CTP acquisitions. Tmax thresholds were 15.2 and 13.7 seconds for GM/WM and the basal ganglia, respectively. Agreement between the SPIRAL and Tmax infarct volume and follow-up DWI infarct volume was tested by calculating the systematic error (bias) and the 95% limits of agreement, defined as the bias ± 1.96 SDs of the individual differences.[15]

We also performed a 10-fold cross-validation for the SPIRAL map (derived from our logistic regression). The analysis was performed on the cohort-level histograms using a 10-fold cross-validation to assess the performance and consistency of the SPIRAL map. Each training set formed 90%, with replacement, of the total population and trained the ROC analysis to determine an optimal threshold. That threshold was then applied to the remaining 10% of the total population to assess sensitivity, specificity, AUC, and the optimal threshold. This process was completed 10 times to determine a mean and SD in each of the above metrics.

A 2-sided P value $< .05$ was considered as statistically significant for all statistical tests. All analyses were performed using R (Version 3.2.1; http://www.r-project.org/), STATA (Version13, StataCorp), and Matlab (R2015a, Version 8.5, MathWorks) statistical packages.

RESULTS

Of a total of 80 patients satisfying study inclusion/exclusion criteria, 72 were included in the study. Some patients ($n = 8$) had inadequate registration results due to severe motion in one of the NCCT or mCTA series. Clinical demographics are summarized in Table 1. Median DWI volume was 12 mL (interquartile range, 2.2–41.8 mL). The optimal SPIRAL functional map derived from the logistic regression was generated from the deconvolution T0 and nondeconvolution TTP, CBF, and MTT. This SPIRAL functional map was used in the patient- and cohort-level analyses as well the cross-validation analysis.

If we compared the ROC-AUC in patients with early and late reperfusion for cortical gray matter + white matter infarction, there was no significant difference at the patient-level (0.83 versus 0.84, respectively), cohort-level (0.82 versus 0.81, respectively), or the cross-validation (0.77 versus 0.74, respectively) (Table 2). When we compared the ROC-AUC in patients with early and late reperfusion for basal ganglia infarction, there was no significant difference at the patient-level (0.82 versus 0.84, respectively), cohort-level (0.81 versus 0.80, respectively), or the cross-validation (0.82 versus 0.78, respectively) (Table 3).

Table 1: Admission demographics, site of occlusion, and workflow metrics

Variables	Total ($n = 72$ Patients)
Age (median) (minimum-maximum) (yr)	68 (32–89)
Men (No.) (%)	37 (51.4)
Stroke on awakening (No.) (%)	27 (46.6)
Site of occlusion (No.) (%)	
MCA	29 (40.3)
ACA	3 (4.0)
ICA	16 (22.2)
Tandem	5 (6.9)
Affected hemisphere (No.) (%)	
Right	30 (41.7)
Left	39 (54.2)
Coronary artery disease (No.) (%)	12 (16.7)
Congestive heart failure (No.) (%)	6 (8.3)
Valvular disease (No.) (%)	2 (3.4)
Hypertension (No.) (%)	38 (52.8)
Dyslipidemia (No.) (%)	24 (33.3)
Diabetes (No.) (%)	1 (1.4)
Smoking (No.) (%)	20 (27.8)
Statin (No.) (%)	22 (37.9)
EVT treatment (No.) (%)	72 (100)
tPA (alteplase) treatment (No.) (%)	55 (76)
Reperfusion (TICI 2b/3) (No.) (%)	72 (100)
Blood glucose (median) (minimum-maximum) (mmol)	6 (4.4–20.0)
NIHSS baseline (median) (minimum-maximum)	17 (1–29)
NIHSS 24 hours (median) (minimum-maximum)	6 (0–24)
MR spectroscopy baseline (median) (minimum-maximum)	0 (0–3)
MR spectroscopy (median) (minimum-maximum) (90 days)	2 (0–6)
CT to reperfusion time (median) (minimum-maximum) (hh:mm)	1:28 (0:27–3:06)

Note:—hh:mm indicates hours: minutes; ACA, anterior cerebral artery.

In the patient-level ROC analysis, the SPIRAL map had a slightly higher, though nonsignificant ($P < .05$), average ROC-AUC (cortical GM/WM = 0.83; basal ganglia = 0.79, respectively) than both the CTP Tmax (cortical GM/WM = 0.82; basal ganglia = 0.78, respectively) and CTP-CBF (cortical GM/white matter = 0.74; basal ganglia = 0.78, respectively) parameter maps. The same relationship was observed at the cohort level (Table 4).

Bland-Altman plots display the mean difference from zero and limits of agreement (2 SDs) to compare the SPIRAL and CTP Tmax infarct volume and follow-up DWI infarct volume (Fig 1). The Bland-Altman plots for SPIRAL and CTP Tmax infarct core volume show that the bias of agreement was similar when comparing the 2 techniques. Similar agreement was observed for the SPIRAL and GE-CTP Tmax infarct core volume with 24-hour DWI infarct volume: The SPIRAL and Tmax map (cortical GM/WM) infarct core

Table 2: ROC curve AUC for SPIRAL map, stratified by CT-to-reperfusion time for cortical gray and white matter tissue

Statistic	AUC, Patient Level	AUC, Cohort Level	Cross-Validation Sensitivity	Cross-Validation Specificity	Cross-Validation Accuracy
Early reperfusion, <90 minutes ($n = 48$ patients)					
Mean	0.83	0.82	0.82	0.72	0.77
SD	0.14	NA	0.06	0.03	0.06
Late reperfusion, >90 minutes ($n = 24$ patients)					
Mean	0.84	0.81	0.79	0.70	0.74
SD	0.11	NA	0.08	0.06	0.07

Note:—NA indicates not applicable.

Table 3: ROC curve AUC for SPIRAL map, stratified by CT-to-reperfusion time for basal ganglia regions

Statistic	AUC, Patient Level	AUC, Cohort Level	Cross-Validation Sensitivity	Cross-Validation Specificity	Cross-Validation Accuracy
Early reperfusion, >90 minutes (21 patients)					
Mean	0.82	0.81	0.82	0.81	0.82
SD	0.11	NA	0.05	0.06	0.06
Late reperfusion, <90 minutes (7 patients)					
Mean	0.84	0.80	0.86	0.71	0.78
SD	0.1	NA	0.08	0.09	0.09

Note:—NA indicates not applicable.

Table 4: ROC curve AUC for SPIRAL map comparison with cine CTP maps for a 40-patient subcohort

Statistic	Cortical GM and White Matter (WM)	Basal Ganglia
SPIRAL map		
AUC, patient level (mean) (SD)	0.83 (0.14)	0.79 (0.08)
AUC, cohort level (mean)	0.82	0.80
CTP T-max map		
AUC, patient level	0.82 (0.13)	0.78 (0.11)
AUC, cohort level	0.81	0.74
CTP blood flow map		
AUC, patient level	0.74 (0.14)	0.78 (0.09)
AUC, cohort level	0.72	0.77

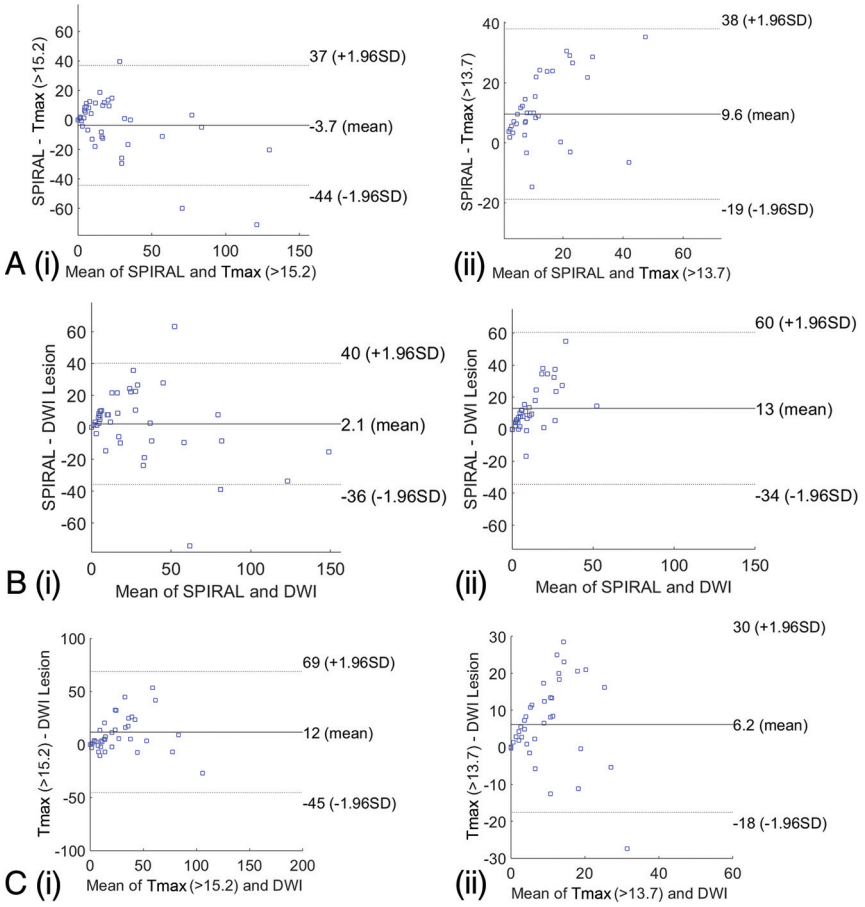

FIG 1. Bland-Altman plots for SPIRAL infarct volume (milliliters) (*A*) and Tmax infarct volume (milliliters) in cortical gray matter/white matter (i) and basal ganglia (ii). SPIRAL infarct volume (milliliters) (*B*) and follow-up DWI infarct volume (milliliters) in the cortical gray matter/white matter (i) and basal ganglia (ii). *C*, Tmax infarct volume and follow-up DWI infarct volume in cortical gray matter/white matter (i) and basal ganglia (ii).

volume mean difference was −3.7 cm^3 (1.96 SDs: −44–37 cm^3); the SPIRAL and Tmax (basal ganglia) infarct core volume mean difference was 9.6 cm^3 (1.96 SDs: −19–38 cm^3). Finally, the SPIRAL infarct core volume (cortical GM/WM) and 24-hour DWI volume mean difference was 2.1 cm^3 (1.96 SDs: −36–40 cm^3) ; the SPIRAL infarct core volume (basal ganglia) and 24-hour DWI volume mean difference was 13 cm^3 (1.96 SDs: −34–60 cm^3).

The SPIRAL map was less accurate in detecting smaller lesions (1–10 mL) while equally as accurate in identifying larger lesions (>100 mL) compared with CTP (Fig 2).

DISCUSSION

Perfusion from low temporally sampled contrast-enhanced imaging has been previously shown in a seminal article by Heinz et al,[16] in 1979. Similarly, we have shown that perfusion parameter maps can be successfully generated from a temporally sampled helical CTA, potentially obviating the need for an additional cine CTP scan in the future. The accuracy, sensitivity, and specificity for follow-up infarct volume is similar to reported values from the CTP literature and the current CTP paradigm available at the authors' institution.[7] Bland-Altman plots showed good agreement between SPIRAL and CTP infarct core volume and for SPIRAL and CTP comparisons with 24-hour DWI follow-up for cortical gray/white matter. The limits of agreement for SPIRAL and CTP Tmax infarct volume were greater for the basal ganglia threshold. In support of our conclusions from this study, we have recently shown that perfusion measured on mCTA source images can better predict follow-up infarction (quantified by the ASPECTS) and clinical outcomes compared with NCCT and mCTA-rLMC (regional leptomeningeal collateral) (pial collateral scoring), the current paradigm used by the Calgary Stroke Program.[17,18] Furthermore, the NCCT and CTA collateral score for stroke decision-making requires expert interpretation, contributing diagnostic uncertainty among nonexperts.[19,20] We now provide an objective, easy-to-interpret, inexpensive, and time-sensitive imaging paradigm to characterize the ischemic lesion at admission with SPIRAL. Figure 3 provides 3 case study examples of SPIRAL versus CTP Tmax functional maps.

Critical to improving patient outcome in patients with acute stroke is fast treatment, high diagnostic accuracy, and confidence among nonexpert physicians because outcomes of patients with stroke are heavily dependent on these factors.

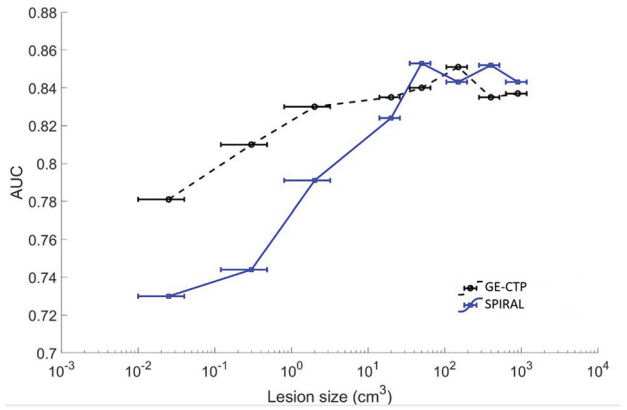

FIG 2. Sensitivity for final infarction on 24-h our MR imaging versus lesion size for SPIRAL and the CTP Tmax map.

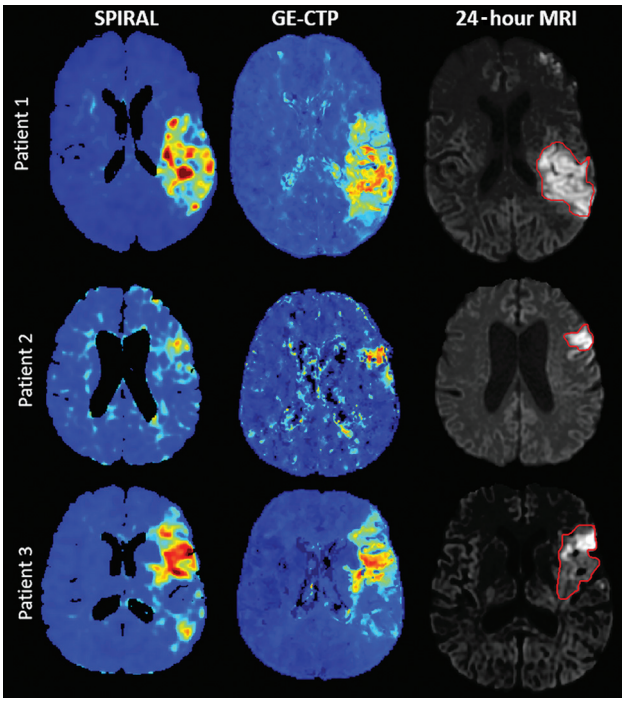

FIG 3. Admission SPIRAL map and CTP Tmax map for 3 patients who underwent EVT for M1 occlusions who had quality/fast reperfusion. The final infarct volume is outlined on the 24-hour DWI.

Brain imaging plays a key role in decision-making that has required expert interpretation,[9,21-28] but among nonstroke experts, it is a major cause for treatment delays.[19,29] CTA is required to identify large-vessel occlusion that may be amenable to removal via EVT. Canadian guidelines strongly recommend the use of CTP to select patients with acute ischemic stroke for EVT in the late time window (6–24 hours after symptom onset).[30] CTP also has the advantage of improving diagnostic accuracy for the identification of ischemic stroke.[31] Although, CTP is a required technique for all Comprehensive Stroke Centers, CTP has significant limitations: It requires separate image acquisition and postprocessing (delaying treatment), another contrast injection (increasing risk of acute nephropathy), and additional exposure to ionizing radiation. Finally, CTP has not been widely adopted in rural stroke centers.[9,32] In this study, we have shown that SPIRAL functional maps can accurately identify infarct core. In its current state, SPIRAL could be used clinically as part of the "perfusion-derived infarct core/clinical penumbra" paradigm for recanalization decision-making, as was shown useful in the Clinical Mismatch in the Triage of Wake Up and Late Presenting Strokes Undergoing Neurointervention With Trevo (DAWN) trial.[4] A prospective study to determine whether SPIRAL is a faster, less expensive, and safer technique for obtaining brain blood flow perfusion maps from a time-resolved helical CT angiogram is warranted.

A few important limitations must be acknowledged. This study has a relatively small sample size of highly selected patients with moderate-to-severe stroke symptoms who were treated with EVT and achieved very good and fast reperfusion. The purpose of these selection criteria was to achieve an operational definition of "infarct core," but we do not know how predictive the SPIRAL map would be in patients with variable reperfusion status and with occlusions in vascular territories other than the anterior circulation. We also had to remove several patients due to the inability to register the images (motion correction to obtain the time-attenuation curve). Nevertheless, the number of patients removed due to this error is consistent with other studies.[7] We also did not separate our gray and white matter tissue compartments to determine respective accuracies; compared with CTP in which an "average map" provides adequate gray/white differentiation, a low temporally resolved CTA cannot provide this. In the future, mCTA perfusion will need to be assessed in a more heterogeneous stroke cohort to determine the relationship between SPIRAL and other commercialized software. We propose that standardized SPIRAL automation will maintain the diagnostic accuracy of cine CTP–based paradigms, thus providing the potential for supporting significant improvements in stroke triage, both in comprehensive and primary stroke centers.

CONCLUSIONS

We have shown that CT perfusion maps can be generated from a temporally sampled helical CTA, potentially replacing a cine CTP scan for triage of patients with ischemic stroke. SPIRAL has the potential for reducing the time for image acquisition and radiologic interpretation compared with NCCT, CTA collateral scores, and cine CT perfusion techniques.

ACKNOWLEDGMENTS

The authors would like to thank the Calgary Stroke Program and Seaman Family MR Research Centre staff for helping with this study.

Disclosures: Commor McDougall—*UNRELATED*: *Comments*: stock ownership in Andromeda Medical Imaging Inc. Andrew M. Demchuk—*UNRELATED*: *Employment*: University of Calgary; *Patents (Planned, Pending or Issued)*: Circle NVI, *Comments*: imaging software; *Stock/Stock Options*: Circle NVI, *Comments*: imaging software. Nils Daniel Forkert—*UNRELATED*: *Grants/Grants Pending*: Natural Sciences and Engineering Research Council of Canada, Canada Research Chair.* Michael D. Hill—*UNRELATED*: *Board Membership*: CNS Foundation, Circle NVI, *Comments*: unpaid, stock ownership in Circle NVI; *Consultancy*: NoNo, *Comments*: unpaid; *Grants/Grants Pending*: Stryker, Medtronic, NoNo, Boehringer Ingelheim, *Comments*: grants for clinical trials*; *Patents (Planned, Pending or Issued)*: US Patent office No. 62/

086,077; *Stock/Stock Options*: Circle NVI; *Other*: Sun Pharmaceutical Industries, *Comments*: adjudicator for outcomes in clinical trials, safety monitor, paid position. Christopher d'Esterre—*UNRELATED*: *Comments*: stock ownership in Andromeda Medical Imaging Inc. Philip A. Barber—*RELATED*: *Grant*: Canadian Institutes of Health Research grant*; *Consulting Fee or Honorarium:* Ablynx.* *UNRELATED*: *Comments*: stock ownership in Andromeda Medical Imaging Inc. *Money paid to the institution.

REFERENCES

1. Goyal M, Demchuk AM, Menon BK, et al; ESCAPE Trial Investigators. **Randomized assessment of rapid endovascular treatment of ischemic stroke**. *N Engl J Med* 2015;372:1019–30. CrossRef Medline
2. Saver JL, Goyal M, Bonafe A, et al; SWIFT PRIME Investigators. **Stent-retriever thrombectomy after intravenous t-PA vs. t-PA alone in stroke**. *N Engl J Med* 2015;372:2285–95 CrossRef Medline
3. Campbell BC, Mitchell PJ, Kleinig TJ, et al; EXTEND-IA Investigators. **Endovascular therapy for ischemic stroke with perfusion-imaging selection**. *N Engl J Med* 2015;372:1009–18 CrossRef Medline
4. Albers GW, Marks MP, Kemp S, et al; DEFUSE 3 Investigators. **Thrombectomy for stroke at 6 to 16 hours with selection by perfusion imaging**. *N Engl J Med* 2018;378:708–18 CrossRef Medline
5. Haussen DC, Dehkharghani S, Rangaraju S, et al. **Automated CT perfusion ischemic core volume and noncontrast CT ASPECTS (Alberta Stroke Program Early CT Score): correlation and clinical outcome prediction in large vessel stroke**. *Stroke* 2016;47:2318–22 CrossRef Medline
6. Nogueira RG, Jadhav AP, Haussen DC, et al; DAWN Trial Investigators. **Thrombectomy 6 to 24 hours after stroke with a mismatch between deficit and infarct**. *N Engl J Med* 2018;378:11–21 CrossRef Medline
7. d'Esterre CD, Boesen ME, Ahn SH, et al. **Time-dependent computed tomographic perfusion thresholds for patients with acute ischemic stroke**. *Stroke* 2015;46:3390–97 CrossRef Medline
8. Naylor J, Churilov L, Chen Z, et al. **Reliability, reproducibility and prognostic accuracy of the Alberta Stroke Program Early CT Score on CT perfusion and non-contrast CT in hyperacute stroke**. *Cerebrovasc Dis* 2017;44:195–202 CrossRef Medline
9. Menon BK, d'Esterre CD, Qazi EM, et al. **Multiphase CT angiography: a new tool for the imaging triage of patients with acute ischemic stroke**. *Radiology* 2015;275:510–20 CrossRef Medline
10. Konstas AA, Goldmakher GV, Lee TY, et al. **Theoretic basis and technical implementations of CT perfusion in acute ischemic stroke, Part 2: technical implementations**. *AJNR Am J Neuroradiol* 2009;30:885–92 CrossRef Medline
11. Studholme C, Hill DL, Hawkes DJ. **Automated 3D registration of MR and CT images of the head**. *Med Image Anal* 1996;1:163–75 CrossRef Medline
12. Gobbi DG, Peters TM. **Generalized 3D nonlinear transformations for medical imaging: an object-oriented implementation in VTK**. *Comput Med Imaging Graph* 2003;27:255–65 CrossRef Medline
13. Sah RG, d'Esterre CD, Hill MD, et al. **Diffusion-weighted MRI stroke volume following recanalization treatment is threshold-dependent**. *Clin Neuroradiol* 2019;29:135–41 CrossRef Medline
14. Akobeng AK. **Understanding diagnostic tests 3: receiver operating characteristic curves**. *Acta Paediatr* 2007;96:644–47 CrossRef Medline
15. Bland JM, Altman DG. **Statistical methods for assessing agreement between two methods of clinical measurement**. *Lancet* 1986;327:307–10 CrossRef
16. Heinz ER, Dubois P, Osborne D, et al. **Dynamic computed tomography study of the brain**. *J Comput Assist Tomogr* 1979;3:641–49 CrossRef Medline
17. Reid M, Famuyide AO, Forkert ND, et al. **Accuracy and reliability of multiphase CTA perfusion for identifying ischemic core**. *Clin Neuroradiol* 2019;29:543–52 CrossRef Medline
18. Zerna C, Assis Z, d'Esterre CD, et al. **Imaging, intervention, and workflow in acute ischemic stroke: the Calgary approach**. *AJNR Am J Neuroradiol* 2016;37:978–84 CrossRef Medline
19. Shamy MC, Jaigobin CS. **The complexities of acute stroke decision-making: a survey of neurologists**. *Neurology* 2013;81:1130–33 CrossRef Medline
20. Moeller JJ, Kurniawan J, Gubitz GJ, et al. **Diagnostic accuracy of neurological problems in the emergency department**. *Can J Neurol Sci* 2008;35:335–41 CrossRef Medline
21. Wintermark M, Albers GW, Broderick JP, et al; Stroke Imaging Research (STIR) and Virtual International Stroke Trials Archive (VISTA)-Imaging Investigators. **Acute stroke imaging research roadmap II**. *Stroke* 2013;44:2628–39 CrossRef Medline
22. Goyal M, Menon BK, Derdeyn CP. **Perfusion imaging in acute ischemic stroke: let us improve the science before changing clinical practice**. *Radiology* 2013;266:16–21 CrossRef Medline
23. Sheth KN, Terry JB, Nogueira RG, et al. **Advanced modality imaging evaluation in acute ischemic stroke may lead to delayed endovascular reperfusion therapy without improvement in clinical outcomes**. *J NeuroIntervent Surg* 2013;5:i62–65 CrossRef Medline
24. Menon BK, Almekhlafi MA, Pereira VM, et al; STAR Study Investigators. **Optimal workflow and process-based performance measures for endovascular therapy in acute ischemic stroke: analysis of the Solitaire FR Thrombectomy for Acute Revascularization study**. *Stroke* 2014;45:2024–29 CrossRef Medline
25. Kudo K, Sasaki M, Yamada K, et al. **Differences in CT perfusion maps generated by different commercial software: quantitative analysis by using identical source data of acute stroke patients**. *Radiology* 2010;254:200–09 CrossRef Medline
26. Bivard A, Levi C, Spratt N, et al. **Perfusion CT in acute stroke: a comprehensive analysis of infarct and penumbra**. *Radiology* 2013;267:543–50 CrossRef Medline
27. Nambiar V, Sohn SI, Almekhlafi MA, et al. **CTA collateral status and response to recanalization in patients with acute ischemic stroke**. *AJNR Am J Neuroradiol* 2014;35:884–90 CrossRef Medline
28. Mishra SM, Dykeman J, Sajobi TT, et al. **Early reperfusion rates with IV tPA are determined by CTA clot characteristics**. *AJNR Am J Neuroradiol* 2014;35:2265–72 CrossRef Medline
29. Barber PA, Zhang J, Demchuk AM, et al. **Why are stroke patients excluded from tPA therapy? An analysis of patient eligibility**. *Neurology* 2001;56:1015–20 CrossRef Medline
30. Boulanger JM, Lindsay MP, Gubitz G, et al. **Canadian stroke best practice recommendations for acute stroke management: prehospital, emergency department, and acute inpatient stroke care, 6th edition, update 2018**. *Int J Stroke* 2018;13:949–84 CrossRef Medline
31. Hoang JK, Wang C, Frush DP, et al. **Estimation of radiation exposure for brain perfusion CT: standard protocol compared with deviations in protocol**. *AJR Am J Roentgenol* 2013;201:W730–34 CrossRef Medline
32. Davenport MS, Khalatbari S, Dillman JR, et al. **Contrast material-induced nephrotoxicity and intravenous low-osmolality iodinated contrast material**. *Radiology* 2013;267:94–105 CrossRef Medline